A Novel $\mathcal{D}$-Metric for Blind Detection of Polar Codes

Yuqing Ren[1,2,3,4], Feng Shu[4,*], Liping Li[5], Zaichen Zhang[2,3], Xiaohu You[1], and Chuan Zhang[1,2,3,*]

[1]Lab of Efficient Architectures for Digital-communication and Signal-processing (LEADS)
[2]National Mobile Communications Research Laboratory, Southeast University
[3]Quantum Information Center of Southeast University, Nanjing, China
[4]School of Electronic and Optical Engineering, Nanjing University of Science and Technology, Nanjing, China
[5]School of Electronics and Information Engineering, Anhui University, Hefei, China
Email: {yqren, shufeng}@njust.edu.cn, chzhang@seu.edu.cn, liping_li@ahu.edu.cn

***Abstract*—As a known error-correcting code that has been proved to fully achieve the binary discrete memoryless channel (B-DMC) capacity, polar codes have been considered as a breakthrough in coding theory since its invention. In 2016, polar codes were selected by the 3GPP as the control channel codes for the enhance mobile broadband (eMBB) scenario. The related research of polar codes has been further pushed to the forefront of applications. In spite of the urgent practical needs, research on the algorithm design and efficient implementation of polar codes for control channels and Internet of Things (IoT) is still in infancy. This paper is to combine successful cancellation (SC) and simplified successful cancellation (SSC) decoders to propose a low-complexity algorithm that can realize blind detection of polar codes. Log-likelihood ratios (LLRs) of frozen bits are used to introduce a new metric $\mathcal{D}$, which is to distinguish polar codes of different formats. The realization of blind detection of polar codes can avoid the receiver's executing complicated decoding algorithm for all polar code candidates, reducing the power, complexity, and delay.**

***Index Terms*—Polar codes, blind detection, metric $\mathcal{D}$, simplified successful cancellation (SSC)**

I. Introduction

In modern communications, such as LTE/LTE-A, blind detection allows user equipments (UEs) to get control information of downlink. In general, control information is protected by channel codes and cyclic redundancy checks (CRC). UEs will try to decode candidates to find the control information according to the combination of system parameters. Actually, traversing the entire candidate space is quite complicated for UEs. In order to meet the efficiency requirement of 5G [1], it is important to improve efficiency and reduce decoding attempts for blind detection[2].

Polar codes are capacity-achieving and of low decoding complexity. In [3], successful cancellation (SC) decoding is proposed by Arıkan. Then, [4] combined SC list (SCL) decoding [5] and CRC, to achieve comparable performance as low-density parity-check (LDPC) codes. Recognizing that SC decoding steps are redundant for some bits, which can be alternatively estimated at the same time, [6] proposed simplified SC (SSC) decoding. Belief propagation (BP) is considered for high-speed applications due to its high parallelism [7].

In existing mobile communications, blind detection is offered by several solutions. The method applied in LTE relies on the concatenation of CRC and convolutional codes. Besides, there are other blind detection algorithms for different codes, such as Bose-Chaudhuri-Hocquenghem (BCH) codes [8] and LDPC codes [9]. However, since the control information specified in 5G will be encoded by polar codes [10], the research of blind detection of polar codes is particularly prominent. Currently, [11, 12] have initially proposed blind detection of polar codes.

In this paper, we utilize the ideas of [11, 12] based on SC and SSC algorithms, and propose a simple blind detection of polar codes by accumulating likelihood ratios of specific bits. From the simulation results, we can see that polar codes and non-polar codes are well separated with respect to metric $\mathcal{D}$. Moreover, in the case of known code rate and unknown code length, this method can distinguish different polar codes. Fig. 1 is the framework of the proposed blind detector.

The rest of this paper is organized as follows. Section II reviews existing algorithms and implementations of polar codes. Simple blind detection is given in Section III. Section IV gives simulation results of different signals with the proposed algorithm. Conclusions are drawn in Section V.

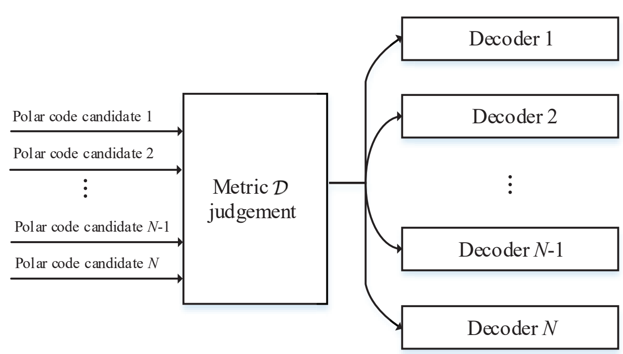

Fig. 1. Framework of the simple blind detection decoder.

II. Polar Codes

A. Preliminaries of Polar Codes

Polar codes are proposed based on the channel polarization phenomenon [3], which means that the performance of binary channels is extremely distributed after N separated channels are merged and split. Some channels become perfectly good channels, and some become completely poor channels. In this way, when $N \to +\infty$, channel capacity will approach the Shannon limit. Therefore, good channels are selected to transmit information bits, bad channels to transmit redundant information[13].

For (N, k) polar code, we select channels with high capacity to transmit information bits $u_{\mathcal{A}}$, where $\mathcal{A}$ is a set of information bits. The remaining bits are treated as frozen bits, denoted as $u_{\mathcal{A}^c}$, which are complements of $\mathcal{A}$. Usually, $(N, K, \mathcal{A}, u_{\mathcal{A}^c})$ is used to represent polar codes. Polar codes are encoded as follows [3]

$$x = uF^{\otimes \log_2^N}, F = \left[\begin{smallmatrix} 1 & 0 \\ 1 & 1 \end{smallmatrix}\right], \tag{1}$$

where Fig. 2 is the construction of $N = 16$ polar codes.

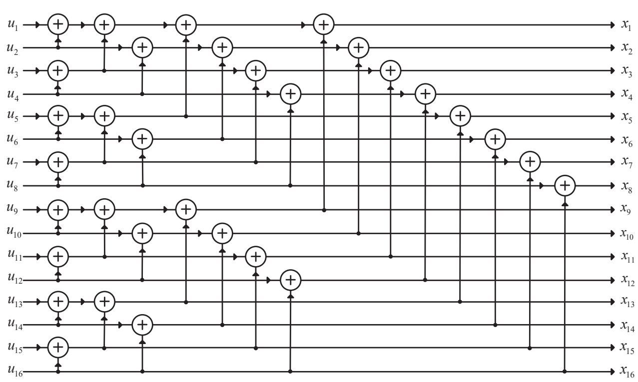

Fig. 2. Construction of polar codes with $N = 16$.

B. SC Decoding Algorithm

Arıkan proposes a low-complexity, successive-cancellation (SC) decoding algorithm [3] for polar codes to sequentially estimate information bits $\hat{u}_i, 1 \le i \le N$. We use the channel output vector y_1^N and the value of previous $i-1$ estimations $\hat{u}_1^{i-1}$ to calculate $\hat{u}_i$, according to Eq. (2)

$$\hat{u}_i = \begin{cases} h(y_1^N, \hat{u}_1^{i-1}), \text{ if } i \in \mathcal{A}, \\ u_i, \text{ if } i \in \mathcal{A}^c, \end{cases} \tag{2}$$

where u_i is a frozen bit, and usually set as 0.

In order to make the SC decoding algorithm more realistic, LLR is often calculated in the logarithmic domain as follows

$$\lambda_{u_0} = \operatorname{sgn}(\lambda_{v_0}) \operatorname{sgn}(\lambda_{v_1}) \min(|\operatorname{sgn}(\lambda_{v_0})|, |\operatorname{sgn}(\lambda_{v_1})|). \tag{3}$$

$$\lambda_{u_1} = g(\lambda_{v_0}, \lambda_{v_1, \hat{u}_0}) = \begin{cases} \lambda_{v_0} + \lambda_{v_1}, \text{ when } \hat{u}_0 = 0; \\ -\lambda_{v_0} + \lambda_{v_1}, \text{ when } \hat{u}_0 = 1. \end{cases} \tag{4}$$

C. SCL Decoding Algorithm

Since SC decoding has a problem of error propagation, [5] proposed the SCL decoding algorithm. The core idea of this algorithm is to change the method that only allows the next expansion from the best one path in the SC decoding to allow the expansion from the best L paths, where $L > 1$ is the search width. After each layer of the path is entirely completed, the Path Metric (PM) established by the algorithm is accumulated once, and the smallest L paths will be stored in a list, waiting for the next expansion[14]. The original idea of the accumulation of metric $\mathcal{D}$ in this paper is derived from SCL. Moreover, PM is defined as follows:

$$\mathrm{PM}_l^{(i)} \approx \begin{cases} \mathrm{PM}^{(i-1)}, \text{ if } \hat{u}_i[l] = \delta(L_N^{(i)}[l]); \\ \mathrm{PM}^{(i-1)} + |L_N^{(i)}[l]|, \text{ if } \hat{u}_i[l] \neq \delta(L_N^{(i)}[l]). \end{cases} \tag{5}$$

where $\delta(x) = (1 - \operatorname{sgn}(x))/2$, $\mathrm{PM}_l^{(0)} = 0$.

D. SSC Decoding Algorithm

SSC algorithm proposed in [6] can reduce the SC decoding delay by in-place binary decision. According to the dependent relationship between bit decisions of polar codes under SC decoding, a code tree $\Gamma = (\varepsilon, \mathcal{V})$ can be constructed from the structure of Fig. 2, where ε and $\mathcal{V}$ respectively represent edge set and node set in the code tree. For a code length of N, the node set $\mathcal{V}$ can be divided into $\log_2 N + 1$ subsets according to the node depth, denoted as $\mathcal{V}_d$, where $d = 0, 1, \ldots, \log_2 N$. In particular, $\mathcal{V}_0$ contains only one root node, i.e. $|\mathcal{V}_0 = 1|$, and all other nodes except leaf nodes are connected respectively to the successors in the two $\mathcal{V}_{d+1}$ by edges marked 0 and 1. In fact, the code tree structure is only related to N. The decoding process is to find a suitable path on the full binary tree. For node v, the length of corresponding component code is N_v. In [5], the soft information input vector α_v is obtained from the parent node, and it will calculate α_l to the left-child through the Eq. (3). After the left-child returns the hard decision vector β_l, node v continues to calculate the right-child's soft information input α_r. When the right-child returns the hard decision vector β_r [6], the hard decision vector β_v of the node v is calculated using the following Eq. (6):

$$\beta_v[i] = \begin{cases} \beta_l[i] \oplus \beta_r[i], \text{ when } i < N_v/2; \\ \beta_r[i - N_v/2], \text{ otherwise.} \end{cases} \tag{6}$$

SSC decoding proposes a new division for polar codes, dividing the nodes into Rate-0 nodes N^0, Rate-1 nodes N^1, single-parity-check nodes N^{SPC}, and repetition nodes N^{REP}, which can be used to clip the SC coding tree. Fig. 3(a) shows the SC coding tree of an $(8, 5)$ polar code. After the SSC clips, the code tree changes to Fig. 3(b).

III. Proposed Simple Blind Detection

A. Gaussian Approximation of Polar Codes

Gaussian approximation (GA) [15] is a simplified method for density evolution and has been widely used in LDPC codes [16]. It is used in polar codes coding to estimate the reliability of the channel [17], i.e., the error probability of each

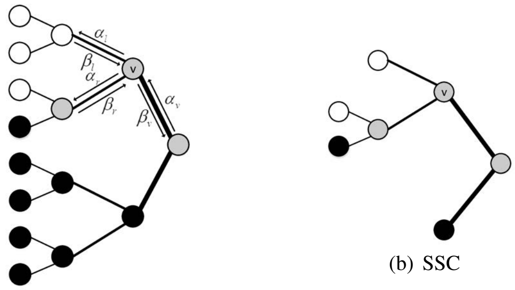

(a) SC

(b) SSC

Fig. 3. Decoder trees corresponding to the SC and SSC algorithms.

polarization channel. The base of applying the GA is that the channels satisfy the symmetry condition, so it conforms to the polar code channels. The GA assumes that each LLR of sub-channels is a gaussian distribution whose variance is double of mean, i.e., $L_N^{(i)} \sim N(m_N^{(i)}, 2m_N^{(i)})$[18].

In the GA structure theory [15], the calculation of density evolution can be transformed into a recursive calculation of the mean $m_N^{(i)}$:

$$m_{2N}^{(2i-1)} = \varphi^{-1}(1 - [1 - \varphi(m_N^{(i)})]^2) \tag{7}$$

When the code length N of polar codes is very long, due to the calculation error of the formula $\varphi(x)$ will bring a large performance loss, so [19] proposed an improved approximate version of GA (AGA). It uses the cumulative-logarithmic error (CLE) to quantify the residual error of AGA in the log-domain, and proposes a new three-stage function:

$$\varphi_{AGA-3}(x) = \begin{cases} e^{0.06725x^2 - 0.4908x}, \ 0 < x < \alpha; \\ e^{-0.4527x^{0.86} + 0.0218}, \ \alpha < x < \beta; \\ e^{0.2832x - 0.4254}, \ \beta < x. \end{cases} \tag{8}$$

B. Simple Blind Detection Rules

Now we introduce a low-complexity algorithm for blind detection of polar codes, and propose a reasonable decoder structure. The blind detection of polar codes is actually setting up a metric $\mathcal{D}$ by researching the special association during the decoding process, in case of lacking all or part of prior information of encoded signals. Then we perform threshold detection on this metric $\mathcal{D}$ to achieve blind detection of polar codes.

Mentioned in [9], blind detection of LDPC code is performed by using a parity check matrix. However, in the absence of any priori information, i.e., full blindness, it is impractical to recover a large parity check matrix. Therefore, the transceiver needs to predefine the set of modulation\encoding, and the set of candidates is known to both receivers and transmitters. The method of simple blind detection designed in this section also uses the idea above. The receivers store some priori information of the polar codes candidates in advance, such as the code length and code rate of each candidate. In the process of decoding, similar to accumulation of PM value in SCL [5], metric $\mathcal{D}$ is continuously accumulated. Finally, we will find the correct encoding format from the candidate set by the value of $\mathcal{D}$, then perform correct decoding.

To perform blind detection for the received information, we must use a detection metric $\mathcal{D}$ that is sensitive enough to feel the changes of received information y_1^N. Since as the code length N increases, the value of the transition probability function will become smaller and smaller, and the decoder is under the risk of underflow. Therefore before adding the previous metric $\mathcal{D}$, we need to add a mapping relationship:

$$\mathbb{L}_{\text{sym}} = \text{sgn}[\mathbb{L}_N^{(i)}(y_1^N, \hat{u}_1^{i-1})] = \begin{cases} 1, \text{ if } w_0 \geq w_1; \\ -1, \text{ if } w_0 < w_1. \end{cases} \tag{9}$$

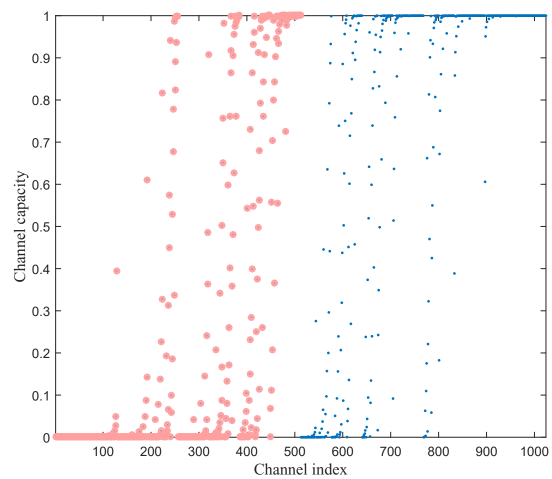

Fig. 4. Channel polarization simulation with N=1024.

Because the absolute value of LLR is greatly influenced by the structure of the decoder, so we require the mapping relationship to eliminate this affect. In this way, the center of gravity of the detection can be attributed to the received information itself. In addition, when calculating the accumulation, the LLRs of information nodes are discarded because the information nodes do not have information redundancy, and only the LLRs of frozen nodes are used for the accumulation. That is, the ratio information of N^0 will be retained and the ratio information of N^1 will be discarded in SSC decoding. Actually, several different nodes are involved in [11], but we abandon N^{SPC} and N^{REP} to propose a new simplified metric.

$$\mathcal{D}[i] = \begin{cases} \mathcal{D}[i-1] + \mathbb{L}_{\text{sym}}, \text{ if } (i \in \mathcal{A}^c) \cap (i \in [1, N_{\text{stop}}]), \\ \mathcal{D}[i-1], \text{ otherwise}, \end{cases} \tag{10}$$

where $\mathcal{D}[0]$ is equal to 0, and N_{stop} is an artificially controllable number of end.

Analyzing the coding structure of polar codes, Fig. 4 is the channel capacity distribution of the polar code with $N = 1024$. From the above, it can be generally known that the detection metric $\mathcal{D}$ should continue to increase positively when calculating channels from 0 to 300. Therefore, we can estimate that the current code length is $N = 1024$ when $\mathcal{D}$ exceeds a certain value d_A. If we continue to accumulate $\mathbb{L}_{\text{sym}}$ at this time, a large number of information bits will intervene, causing a slowdown in the growth of the metric $\mathcal{D}$ or even stopping the increase. After a large number of simulations for polar codes with different code length, their $\mathcal{D}$ will fall in different intervals after threshold detection. The formula is as follows:

$$\mathcal{H} = \begin{cases} \mathcal{H}_1(N=2), \text{ if } \mathcal{D} < d_1; \\ \mathcal{H}_2(N=4), \text{ if } d_1 < \mathcal{D} < d_2; \\ \dots \\ \mathcal{H}_n(N=2^n), \text{ if } d_{n-1} < \mathcal{D} < d_n. \end{cases} \tag{11}$$

C. Structure of Simple Blind Detection

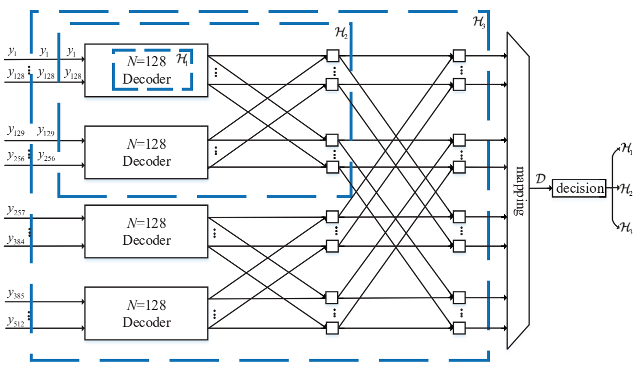

Fig. 5. Structure of simple blind detection decoder.

In combination with the above ideas, we will propose the structure of simple blind detection. Involving the mapping relations $\mathbb{L}_{\text{sym}}$ and accumulation of metric $\mathcal{D}$, this algorithm mainly focuses on the study of LLRs of Rate-0 N^0. Therefore, the decoding structure is improved on the basic of SSC decoding, adding the mapping and decision process.

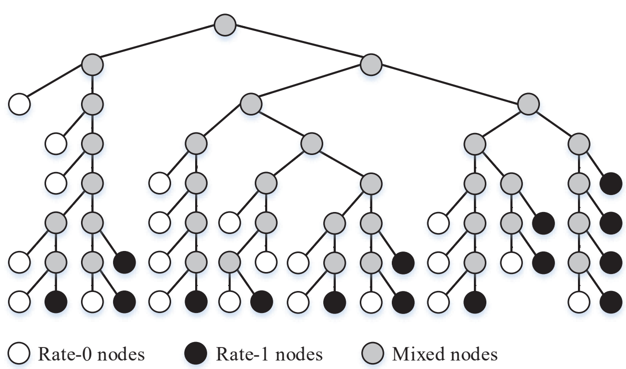

Fig. 6. Decoder-tree representation of a $(128, 32)$ polar code.

As shown in Fig. 5, it is the blind detection structure for polar codes with $N = 128$, $N = 256$, and $N = 512$. When the format information of the received signals is not known for the decoder, we firstly assume that the received information is a polar code with $N = 512$ and send codes to the front-end for decoding. According to the previously stored information of frozen bits position in the receiver, the accumulation of metric $\mathcal{D}$ is performed. In addition, the final decision plays a gating effect. According to the output result, the polar code decoder with correct code length will be selected. This method utilizes the folding feature of polar code decoders, which can greatly simplify the structure of the blind detection decoder.

IV. Numerical Results

In this section, we will present practical and effective simulation results under the additive white Gaussian noise (AWGN) channels. It mainly tests the probability distribution function and probability density function of metric $\mathcal{D}$ with different formats of polar codes and analyzes the error probability after passing the blind detection decoder.

A. Assumptions and Conditions

In 3GPP RAN1 meeting decision, such as reported in [10, 20], polar code which has code length $N_{\max} = 512$ and a low code rate R (generally $1/8$) is often used, so we set code rate R of the tested polar codes as $1/8$. The simulation setting is that polar codes with different code length N pass through the blind detection decoder at the same time, then receivers will detect their code length N in case of known code rate R. We set the three formats of polar codes with $N = 512$, $N = 256$, $N = 128$, $R = 1/8$. The structure of the decoder is actually shown in Fig. 5. In final, all simulation results are used with the binary phase-shift keying (BPSK) modulation over the AWGN channel.

Since this method is based on SC and SSC decoding, it is actually using Rate-0 nodes N^0 and Rate-1 nodes N^1 to clip the SC decoding tree. In consideration of simplifying the algorithm, so the simple blind detection doesn't involve the N^{SPC} and N^{REP}. In general, the algorithm complexity should be somewhere in between. Fig. 6 is the clipping result of $(128, 32)$ polar codes. It can be observed from the Fig. 6 that the original huge binary tree has been simplified enough after trimming the Rate-0 nodes N^0 and Rate-1 nodes N^1.

B. Simulation Results

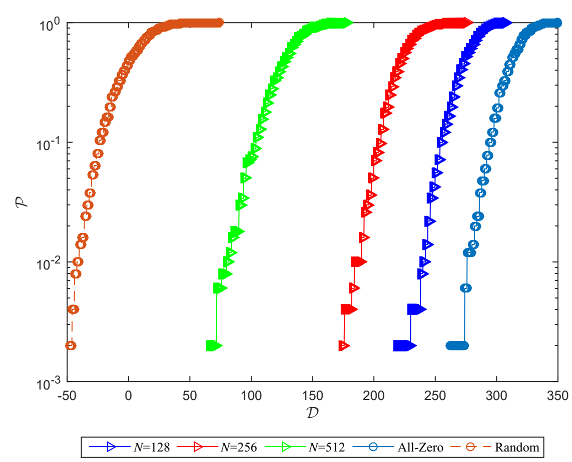

Fig. 7. Probability distribution function of different signals.

The simulation result is performed under the environment that signals go through the AWGN channel with $E_b/N_0 = 2$

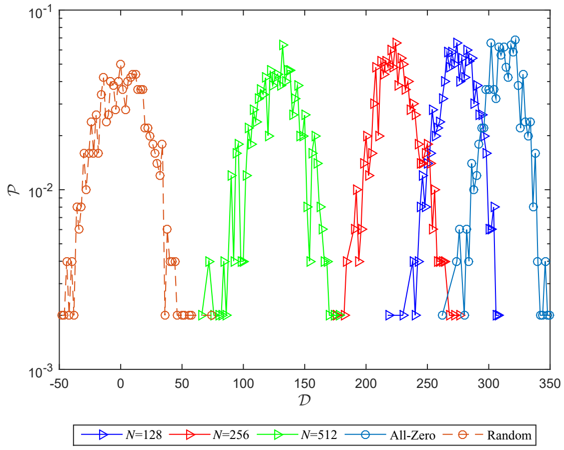

Fig. 8. Probability density function of different signals.

dB after passing the BPSK modulation. As shown in Fig. 7, there are five kinds of signals. In the order of arrangement, they are probability distribution functions of metric $\mathcal{D}$: random signals, $(512, 64)$ polar code, $(256, 32)$ polar code, $(128, 16)$ polar code, and all-zero signals. According to Eq.s (9) and (10), $L_N^{(i)}$ will be mapped to accumulate metric $\mathcal{D}$ when the frozen bits Rate-0 N^0 are decoded.

1) Firstly, we analyze the $(512, 64)$, $(256, 32)$, $(128, 16)$ polar codes images. From the Fig. 7, the accumulation of metric $\mathcal{D}$ is increasing in descending order of code length N, and they are separated well in the metric $\mathcal{D}$ dimension. Based on the original idea, if three kinds of polar codes with different length N pass through the $(512, 64)$ decoder together, as shown in Fig. 5, the $(512, 64)$ polar code should get more frozen bits $\mathbb{L}_{\text{sym}}$ theoretically, so that its speed should be far beyond the polar codes with $N = 256$, 128 when we accumulate the first 384 bits of the $(512, 64)$ decoder.

Since polar codes with $N = 256$, 128 will inject a large number of information bits into the corresponding bits when being decoded by $(512, 64)$ decoder. The information bits are not controllable, resulting in the stagnation or even retrogression of the $\mathcal{D}$ value. However, the simulation results are just contrary to the theory. The reason for this phenomenon is that after channel polarization, the channel capacity for transmitting frozen bits is close to 0 and the channel quality is extremely poor. If we don't judge directly by the prior information $\mathcal{A}^c$ when we transmit 0 in frozen bits, most of them will be translated into 1 at the decoding end. Therefore, it explains how the metric $\mathcal{D}$ increases as the code length N decreases.

2) Next we will analyze random signals and all-zero signals. Random signals is the random sequences which we transmit at the transmit end without any polar code encoding format. Similarly, all-zero signals refer to sending all-zero sequences without any polar code encoding format at the transmitter. According to Fig. 7, the metric $\mathcal{D}$ of random signals is basically distributed around 0 and well distinguished from the other three polar codes signals, which is consistent with the characteristics of the random signals. All-zero signals are distributed on the far right side of the image, so the accumulation speed of the metric $\mathcal{D}$ is the fastest. This phenomenon is also in line with its own performance.

TABLE I
DISTRIBUTION RANGE OF METRIC $\mathcal{D}$ FOR DIFFERENT POLAR CODES.

E_b/N_0 (dB)	$(512, 64)$ code	$(256, 32)$ code	$(128, 16)$ code
0.5	$(68, 178)$	$(152, 262)$	$(220, 302)$
1	$(68, 182)$	$(154, 258)$	$(218, 308)$
2	$(66, 178)$	$(174, 276)$	$(222, 314)$
3	$(76, 182)$	$(182, 276)$	$(242, 322)$
4	$(62, 190)$	$(192, 278)$	$(250, 332)$

In order to show the differences better in the metric $\mathcal{D}$ distribution of different signals, we use the probability density function to display more directly. As shown in Fig. 8, the metric $\mathcal{D}$ of five kinds of signals shows obviously sharp peaks, among which the random signals and the three polar codes are particularly distinct under the simple blind detection algorithm. According to Eq. (12), False Alarm and Miss Alarm rate of blind detection are

$$\begin{cases} P_{false}(\mathcal{H}_i) = \sum\limits_{j \neq i} P(\mathcal{H}_j|\mathcal{H}_i)P(\mathcal{H}_i); \\ P_{miss}(\mathcal{H}_i) = \sum\limits_{j \neq i} P(\mathcal{H}_i|\mathcal{H}_j)P(\mathcal{H}_j). \end{cases} \tag{12}$$

In addition, except for the final all-zero signals, the peaks of metric $\mathcal{D}$ are all well distinguished in Fig. 8, so the probability of calculating False Alarm and Miss Alarm is actually only related to adjacent peaks, i.e., we can add the restrictions to Eq. (12), such as $i - 1 \leq j \leq i + 1$.

C. Improved Results

In order to make the simple blind detection algorithm more adaptable to the reality, we simulate at different E_b/N_0 and focus on the distinction between three different polar codes. Table. I is the metric $\mathcal{D}$ distribution range of three polar codes at different E_b/N_0. It can be seen from the table that as the E_b/N_0 increases, the metric $\mathcal{D}$ is separated more obviously. Moreover, it show a tendency to increase to the right at a certain extent. Therefore, according to Eq. (11), we define the metric $\mathcal{D}$ interval of the three signals as $(60, 190)$, $(191, 264)$, $(265, 330)$, and we can perform frame error rate (FER) simulation based on this.

Fig.9 shows the FER of polar codes with $N = 512$, 256, 128 under the simple blind detection algorithm, where the FER of all-signals refers to sending three kinds of codes randomly at the transmitters and passing the algorithm at the receivers.

V. CONCLUSION

In this paper, we propose a low-complexity blind detection based on the SC and SSC algorithms. Combined with the properties of frozen bits' LLR in the polar decoding, a new

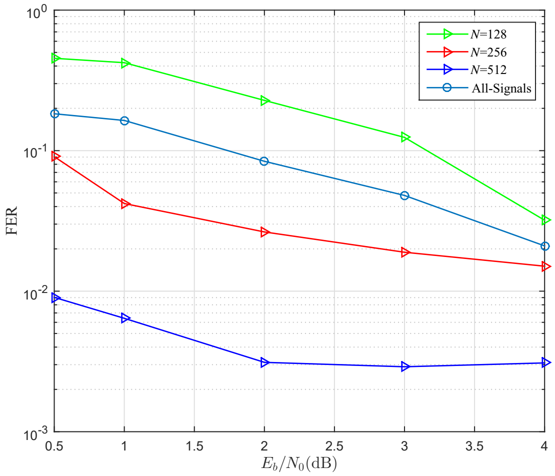

Fig. 9. FER of simple blind detection algorithm.

metric $\mathcal{D}$ is used in blind detection of polar codes in this work. According to the simulation results, $(512, 64)$, $(256, 32)$, $(128, 16)$ polar codes can be distinguished well in the metric $\mathcal{D}$ dimension, which have unknown code length and known code rate. Furthermore, the framework of blind detection decoder is given in the paper. To lower the power consumption and delay of receivers, this algorithm shows advantages for realizing blind detection of polar codes.

Acknowledgement

This work is supported in part by NSFC under grant 61501116, Jiangsu Provincial NSF for Excellent Young Scholars, Huawei HIRP Flagship under grant YB201504, the Fundamental Research Funds for the Central Universities, the SRTP of Southeast University, State Key Laboratory of ASIC & System under grant 2016KF007, ICRI for MNC, and the Project Sponsored by the SRF for the Returned Overseas Chinese Scholars of MoE.

References

[1] 3^{rd} Generation Partnership Project (3GPP), "Physical layer procedures," *3GPP TS 36.213 V.8.2.0*, 2008.

[2] C. Zhang, Y. H. Huang, F. Sheikh, and Z. Wang, "Advanced baseband processing algorithms, circuits, and implementations for 5G communication," *IEEE Journal on Emerging & Selected Topics in Circuits & Systems*, vol. PP, no. 99, pp. 1–1, 2017.

[3] E. Arikan, "Channel polarization: A method for constructing capacity-achieving codes for symmetric binary-input memoryless channels," *IEEE Trans. Inf. Theory*, vol. 55, no. 7, pp. 3051–3073, 2009.

[4] G. Sarkis, P. Giard, A. Vardy, C. Thibeault, and W. J. Gross, "Fast list decoders for polar codes," *IEEE J. Sel. Areas Commun.*, vol. 34, no. 2, pp. 318–328, 2016.

[5] I. Tal and A. Vardy, "List decoding of polar codes," *IEEE Trans. Inf. Theory*, vol. 61, no. 5, pp. 2213–2226, 2015.

[6] A. Alamdar-Yazdi and F. R. Kschischang, "A simplified successive-cancellation decoder for polar codes," *IEEE Commun. Lett.*, vol. 15, no. 12, pp. 1378–1380, 2011.

[7] B. Yuan and K. K. Parhi, "Architecture optimizations for BP polar decoders," in *Proc. IEEE International Conference on Acoustics, Speech and Signal Processing (ICASSP)*, 2013, pp. 2654–2658.

[8] J. Zhou, Z. Huang, C. Liu, S. Su, and Y. Zhang, "Information-dispersion-entropy-based blind recognition of binary BCH codes in soft decision situations," *Entropy*, vol. 15, no. 5, pp. 1705–1725, 2013.

[9] T. Xia and H. C. Wu, "Novel blind identification of LDPC codes using average llr of syndrome a posteriori probability," in *Proc. IEEE International Conference on ITS Telecommunications (ITST)*, 2013, pp. 12–16.

[10] MCC Support, "Final report of 3GPP TSG RAN WG1 #87 v1.0.0," Available:http://www.3gpp.org/ftp/tsgran/WG1RL1/TSGR188/Docs/R1-1701552.zip, Feb. 2017.

[11] P. Giard, A. Balatsoukas-Stimming, and A. Burg, "Blind detection of polar codes," in *Proc. IEEE International Workshop on Signal Processing Systems (SiPS)*, 2017, pp. 1–6.

[12] C. Condo, S. A. Hashemi, and W. J. Gross, "Blind detection with polar codes," *IEEE Commun. Lett.*, vol. PP, no. 99, pp. 1–1, 2017.

[13] X. Liang, Y. She, H. Vangala, X. You, C. Zhang, and E. Viterbo, "An efficient successive cancellation polar decoder based on new folding approaches," in *IEEE International Conference on Asic*, 2017, pp. 1077–1080.

[14] H. Song, S. Zhang, X. You, and C. Zhang, "Efficient metric sorting schemes for successive cancellation list decoding of polar codes," in *IEEE International Symposium on Circuits and Systems*, 2017, pp. 1–4.

[15] S. Y. Chung, T. J. Richardson, and R. L. Urbanke, "Analysis of sum-product decoding of low-density parity-check codes using a Gaussian approximation," *IEEE Trans. Inf. Theory*, vol. 47, no. 2, pp. 657–670, 2001.

[16] G. Li, I. J. Fair, and W. A. Krzymien, "Density evolution for nonbinary LDPC codes under gaussian approximation," *IEEE Trans. Inf. Theory*, vol. 55, no. 3, pp. 997–1015, 2009.

[17] P. Trifonov, "Efficient design and decoding of polar codes," *IEEE Trans. Commun.*, vol. 60, no. 11, pp. 3221–3227, 2012.

[18] L. Li, Q. Wang, Y. Hu, and C. Zhang, "Energy consumption of polar codes for wireless sensor networks," in *International Wireless Internet Conference*, 2017, pp. 140–149.

[19] J. Dai, K. Niu, Z. Si, and J. Lin, "Evaluation and optimization of Gaussian approximation for polar codes," *Proceedings of the American Society for Information Science and Technology*, vol. 51, no. 1, pp. 1–2, 2016.

[20] MCC Support, "Final report of 3GPP TSG RAN WG1 #88 v1.0.0," Available:http://www.3gpp.org/ftp/tsgran/WG1RL1/TSGR188b/Docs/R1-1704172.zip, Apr. 2017.